Bulletin of the Seismological Society of America, Vol. 108, No. 3A, pp. 1414–1426, June 2018, doi: 10.1785/0120170270

Ⓔ

Why Aftershock Duration Matters for Probabilistic Seismic Hazard Assessment

by Shinji Toda and Ross S. Stein

Abstract Most hazard assessments assume that high background seismicity rates indicate a higher probability of large shocks and, therefore, of strong shaking. However, in slowly deforming regions, such as eastern North America, Australia, and inner Honshu, this assumption breaks down if the seismicity clusters are instead aftershocks of historic and prehistoric mainshocks. Here, therefore we probe the circumstances under which aftershocks can last for 100–1000 years. Basham and Adams (1983) and Ebel *et al.* (2000) proposed that intraplate seismicity in eastern North America could be aftershocks of mainshocks that struck hundreds of years beforehand, a view consonant with rate–state friction (Dieterich, 1994), in which aftershock duration varies inversely with fault-stressing rate. To test these hypotheses, we estimate aftershock durations of the 2011 M_w 9 Tohoku-Oki rupture at 12 sites up to 250 km from the source, as well as for the near-fault aftershocks of eight large Japanese mainshocks, sampling faults slipping 0.01 to 80 mm/yr. Whereas aftershock productivity increases with mainshock magnitude, we find that aftershock duration, the time until the aftershock rate decays to the premainshock rate, does not. Instead, aftershock sequences lasted a month on the fastest-slipping faults and are projected to persist for more than 2000 years on the slowest. Thus, long aftershock sequences can misguide and inflate hazard assessments in intraplate regions if misinterpreted as background seismicity, whereas areas between seismicity clusters may instead harbor a higher chance of large mainshocks, the opposite of what is being assumed today.

Electronic Supplement: Tables of background rate estimates as well as the Omori parameters and Omori decay parameters for all aftershock sequences, and figures estimating aftershock duration uncertainty, time-dependent completeness magnitudes for the aftershock sequences, alternative estimates of the Omori decay parameters and aftershock duration, earthquake time series and aftershock durations for three types of mainshocks in the Tohoku area, and M_c dependency of aftershock durations for the Tohoku-Oki aftershocks.

Introduction

Aftershocks are earthquakes for which occurrence frequency decays with inverse time. No other aftershock distinction is robust; in other words, no isolated aftershock can be discriminated from a background shock, a mainshock, or a foreshock. The 1891 M_w 7.4 Nobi earthquake not only gave birth to the seminal discovery by Omori (1894) of the inverse-time decay of aftershocks, but is also one of the world's longest continuously recorded aftershock sequences. Utsu *et al.* (1995) extended Omori's time series of felt earthquakes in the epicentral region of the 1891 event and found that the rate continued to decay more than a century later. Against this backdrop, Basham and Adams (1983) first speculated and Ebel *et al.* (2000) argued that today's clusters of intraplate seismicity in eastern North America and Australia (Fig. 1) could be aftershocks of mainshocks that struck hundreds of years ago. Omori's law can be written as follows:

$$n(t) = \frac{k}{(c+t)^p} \tag{1}$$

$$n = 10^{a-bM},$$

in which n is the number of events, t is time, c and k are constants, p is the Omori decay exponent, a is the productivity, and b is the magnitude–frequency relationship.

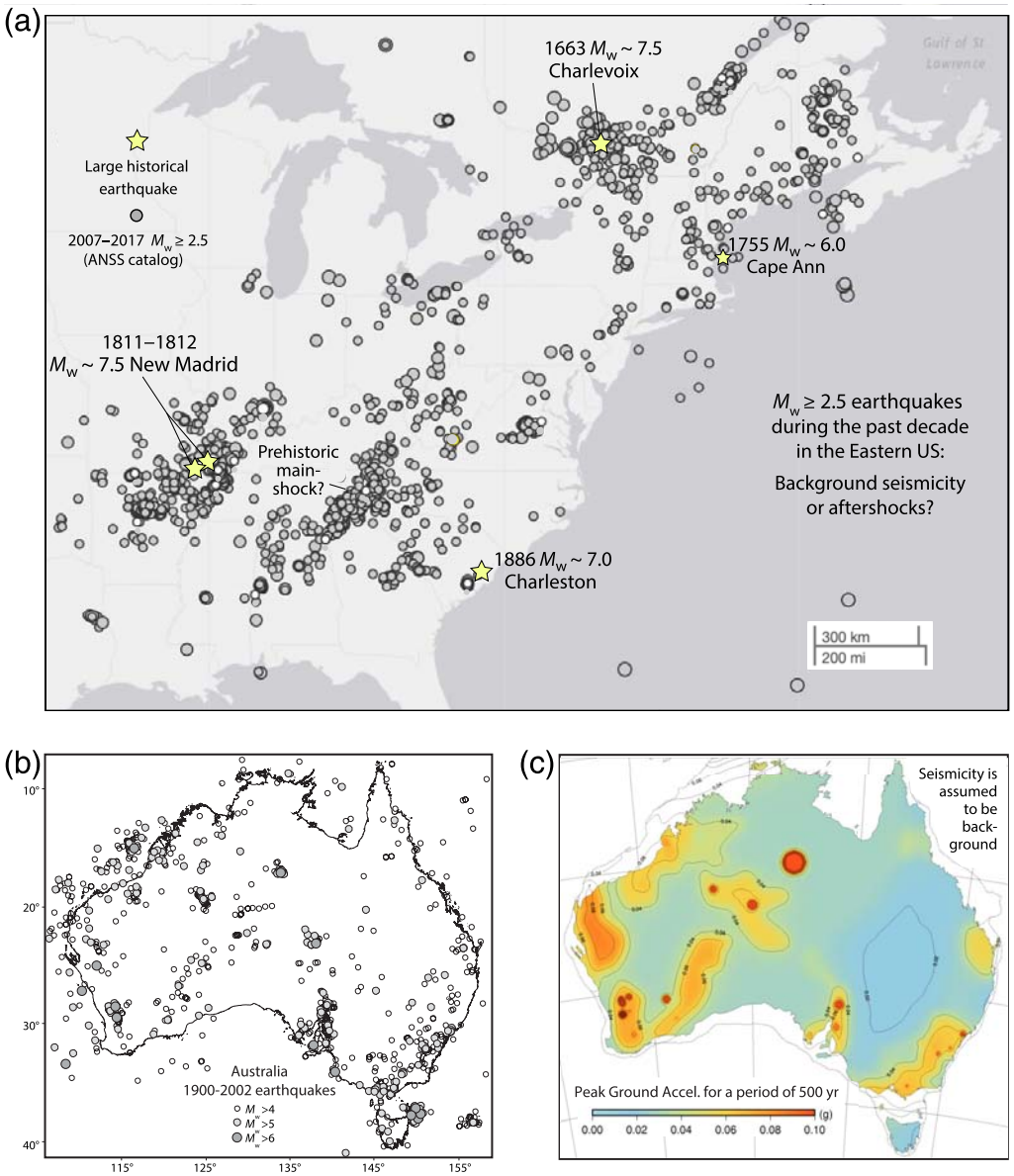

Figure 1. (a) Are these background earthquakes, for which the rates can be scaled up to higher magnitudes for probabilistic seismic hazard assessment, or are they largely aftershocks of rare historic and prehistoric events, in which case their rates will decay, and the likelihood of larger events is diminished? (b,c) The current seismic hazard assessment (Leonard *et al.*, 2013) largely assumes that these events (from Clark and McCue, 2003) are background, in part because the dozen identified active faults are short, isolated, and often show no evidence of displacement for the past 10–30 ka. Therefore, background rates are scaled upward to forecast the probability of strong shaking. The color version of this figure is available only in the electronic edition.

Ebel *et al.* (2000) inferred the times and sizes of mainshocks from historical intensity data, taking the Omori decay exponent p, productivity a, and magnitude–frequency relationship b of the frequency–magnitude distribution from instrumentally recorded California sequences. They calculated the expected rate of $M_w \geq 2$ or ≥ 3 shocks today, contending that much of the current seismicity in stable cratonic regions is aftershocks. But Ebel *et al.* (2000) did not measure the aftershock decay and implicitly assumed that the current seismicity is composed only of aftershocks (in other words, there is no background rate), which need not be the case.

In contrast, two recent studies contend that the long-lived aftershocks cannot explain the contemporary seismicity for the large historical mainshocks that they investigated. On the basis of an epidemic-type aftershock sequence (ETAS) modeling of the current New Madrid, Missouri, earthquakes (Fig. 1a, site of the 1811–1812 M_w ~ 7.4–7.6 shocks), Page and Hough (2014) argued that today's seismicity is background rather than aftershocks. Fereidoni and Atkinson (2014) reached a similar conclusion for seismicity in the St. Lawrence Valley, site of the 1663 M_w ~ 7 Charlevoix earthquake (Fig. 1a), as well as several other smaller events

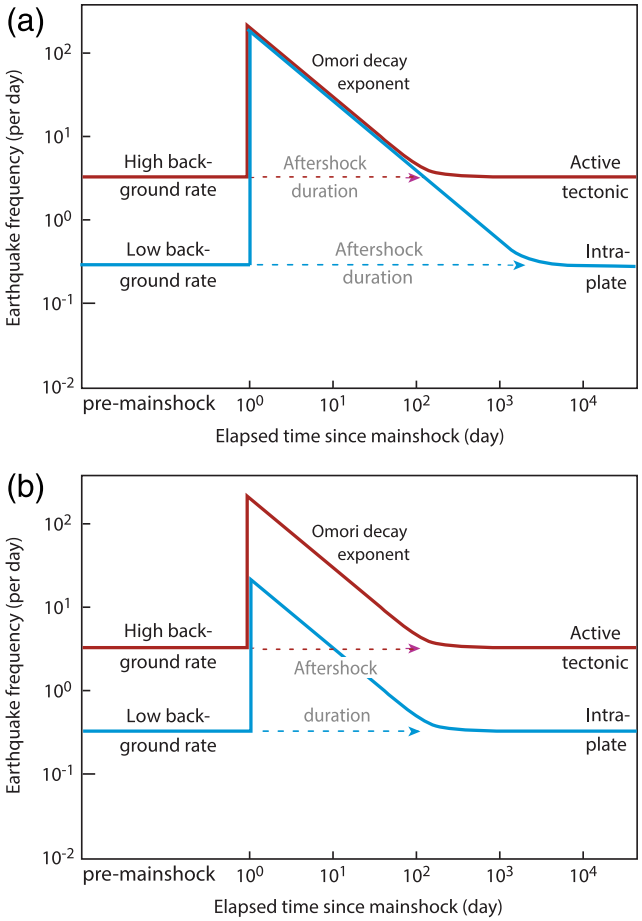

Figure 2. (a) One end member for the dependence of aftershock duration on background rate, here with a fixed Omori decay exponent p for which the apparent duration (the measurable duration) depends on the decay exponent and the background rate. (b) Alternative end member for which background rate plays no role in the apparent aftershock duration. In this case, another factor, such as mainshock magnitude, might dominate. The color version of this figure is available only in the electronic edition.

in southeast Canada. Their data analysis and interpretation are contested by Ebel (2016) and defended by Fereidoni and Atkinson (2016).

In this study, we reassess the Basham and Adams (1983) and Ebel *et al.* (2000) hypotheses by measuring the background seismicity rate and the decay of aftershocks of $7 \le M_w \le 9$ mainshocks in a consistent manner in both rapidly and slowly deforming regions.

Aftershock Duration Could Depend on Stressing or Background Seismicity Rate

A framework for the Ebel *et al.* (2000) hypothesis had already been advanced by Dieterich (1994) when he proposed that aftershock duration t_a should be independent of mainshock magnitude, arguing that

$$t_a = \frac{A\sigma}{\dot{\tau}}, \qquad (2)$$

in which $A\sigma$ is a fault constitutive parameter times the normal stress, and $\dot{\tau}$ is the fault stressing rate. In equation (2), the low stressing rates of intraplate faults would yield long aftershock durations relative to tectonically active faults, as schematically illustrated in Figure 2a. Dieterich (1994) sought to support equation (2) by showing a dependence of aftershock duration on mainshock recurrence times for ten $4.8 \le M_w \le 9.2$ events. But because larger earthquakes tend to have longer recurrence times, Dieterich's plot is equally compatible with aftershock duration governed by mainshock magnitude (Felzer *et al.*, 2004) and so does not test the Basham and Adams (1983) and Ebel *et al.* (2000) hypotheses.

Disputed Eastern North America Aftershocks Compels Use of Japanese Seismicity

Several studies have argued that aftershock behavior is consistent with the Dieterich (1994) hypothesis (Parsons, 2002; Toda *et al.*, 2002, 2005; Toda and Stein, 2002, 2003; Jonsson *et al.*, 2003), whereas Ziv (2006) concluded that aftershock duration is controlled by the extent to which the lower crust is mobilized by the mainshock slip. Stein and Newman (2004) and Stein and Liu (2009) proposed that contemporary seismicity at the sites of the 1811–1812 $M_w \sim 7.4$–7.6 New Madrid earthquakes are aftershocks. The near absence of a measurable strain in New Madrid suggests a very long aftershock duration in the Dieterich relation. Stein and Liu (2009) also examined 16 plate boundary and intraplate earthquakes, estimated their aftershock durations and fault-slip rates, and contended that the durations are consistent with those of the Ebel *et al.* (2000) and Dieterich (1994) hypotheses.

Page and Hough (2014) attempted to generate synthetic catalogs that match the following observations: four mainshocks of M_w 7.0–7.7, two $M_w \ge 6.0$ aftershocks in the first year but none since, and a current rate of 0.3 $M_w \ge 4$ shocks per year. They found that an ETAS sequence active enough to produce the $M_w \ge 6$ shocks in the first few months, as well as the $M_w \le 4$ seismicity rates observed today, would yield too many intervening $M_w \ge 6$ aftershocks. Fereidoni and Atkinson (2014) found that the requisite intermediate magnitude events were also absent at Charlevoix. However, all but the current rate of seismicity is uncertain, and the background rate (in other words, the rate before 1811) is unknown. To us, their argument would be more convincing had they successfully fit the century-long Nobi aftershocks, as well as aftershocks triggered by multiple mainshocks as occurred in 1811–1812, such as the 22 January 1988 M_w 6.3, 6.4, and 6.7 Tennant Creek, Australia (Choy and Bowman, 1990), or the July 1905 M_w 7.9 Tsetserleg and the M_w 8.4 Bolnay, Mongolia, earthquakes that struck 14 days and 100 km apart (Schlupp and Cisternas, 2007).

Therefore, although the Basham and Adams (1983) and Ebel *et al.* (2000) inferences and the Dieterich (1994) theory are compatible, none are confirmed, and the duration of the 1811–1812 New Madrid aftershocks remains under debate. Using the best data available from the standpoint of the

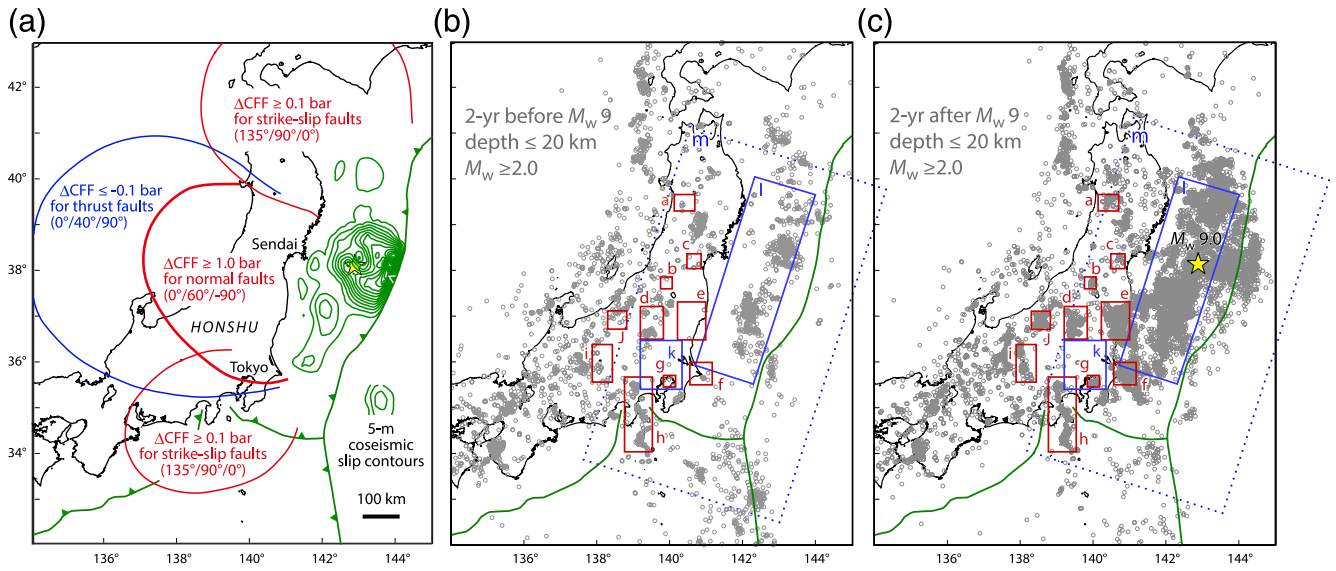

Figure 3. (a) Coulomb stress changes (ΔCFF) imparted by the M_w 9 Tohoku-Oki earthquake (star represents the epicenter) to central Honshu based on the slip model of Iinuma *et al.* (2012). Seismicity during the (b) 2 yrs before and (c) 2 yrs after the M_w 9 Tohoku earthquake, showing the boxes selected for aftershock duration estimation, which are chosen because they exhibit off-fault aftershocks but sample diverse tectonic regimes. Box l is the approximate rupture area of the Tohoku earthquake, and box m encloses the entire area including sites without aftershocks; its decay is shown in Ⓔ Figure S5. The color version of this figure is available only in the electronic edition.

number of well-recorded $M_w \geq 7$ aftershock sequences with low magnitudes of completeness, which lies in Japan, we test not the duration of eastern North American aftershock sequences, but the broader question of whether aftershock duration scales with mainshock magnitude, fault stressing rate, or background seismicity rate. If so, then very long aftershock sequences must be common, even if they cannot be established at New Madrid and Charlevoix. We use the M_w 9 Tohoku, Japan, shock as the trigger for clusters of remote aftershocks to test whether the mainshock magnitude or the stressing rate at the site of the aftershocks governs their duration. We also measure aftershock durations for 10 large mainshocks in northern Honshu, Japan, in different stressing environments.

Duration of Remote Aftershocks of the M_w 9 Tohoku Earthquake

Estimating aftershock duration requires consistent measurement of the background rate and the aftershock zone. The volume that we sampled for aftershocks experienced a calculated stress increase of ≥ 0.1 bar because this is commonly found to be associated with off-fault aftershocks (Harris, 1998). This same volume is used to count background shocks. The importance of these consistent criteria is shown schematically in Ⓔ Figure S1, available in the electronic supplement to this article. What Dieterich (1994) and we refer to as aftershock duration is termed the "apparent aftershock duration" by Hainzl *et al.* (2016).

The M_w 9.0 Tohoku-Oki earthquake caused immediate seismicity-rate changes across much of northern Honshu, which experienced a calculated Coulomb stress change ≥ |0.1 bar| (Fig. 3a; Toda *et al.*, 2011). Close to the Tohoku fault rupture, the stress changes are very large because of the large stress drops (on the order of 100 bars) and because of local spikes in slip; however, far from the fault, the stress changes are still large enough to trigger aftershocks (on the order of 1.0–0.1 bar), even though they are isolated from the 2011 rupture surface. Their isolation could arise because they enclose faults optimally oriented for failure given the stress imparted by Tohoku. In rate–state friction (Dieterich, 1994), any sudden stress increase causes a seismicity jump followed by an Omori decay, regardless of whether it is on or off a fault, as we see here.

We selected the largest concentrations of off-fault seismicity for duration estimation, marked as boxes a–m in Figure 3b,c. To estimate the aftershock duration t_a in each box, we determined the magnitude of completeness M_c as a function of time following Woessner and Wiemer (2005) (Ⓔ Fig. S2, shown with 1-sigma uncertainties), determined the 10-yr background rate μ, and estimated the Omori decay parameters by fitting $k/(t+c)^p$, using the 3-yr period through 31 December 2014 by Monte Carlo estimation (Table 1). In Ⓔ Table S1 and Figure S3, we fit $\mu + k/(t+c)^p$ following Ogata (1998); the results are very similar. We use the 1-sigma ranges of the parameters p, c, and k estimated from the maximum-likelihood method to fit equations (1) and (2). We also consider the standard deviation of the background seismicity rate, performing 1 million realizations to obtain the 34%, 50%, and 68% quantiles of t_a in Table 1. The seismicity time series for each box is shown in Figure 4. These remote Tohoku aftershocks are not simply secondary aftershocks of the first remote aftershocks of Tohoku. In each box, we give the magnitude of the first shock after the M_w 9;

Table 1
Estimated Aftershock Durations for the M_w 9.0 Tohoku-Oki Mainshock

Region	M_c	10-yr Background (/Day)	p-Value	c-Value	k-Value	t_a (in yr, 34% Quantile)	t_a (in yr, 50% Quantile)	t_a (in yr, 68% Quantile)
(a) Southern Akita	1.5	0.037 ± 0.012	1.43 ± 0.05	100 (fixed)	3,809 ± 1,026	7	9	11
(b) Aizu	1.3	0.011 ± 0.008	1.26 ± 0.01	3.84 ± 0.52	8,841 ± 639	108	134	187
(c) Sendai	1.4	0.072 ± 0.048	2.64 ± 0.11	20 (fixed)	2,436,683 ± 1,124,618	2.1	2.7	3.4
(d) Nikko	1.2	0.829 ± 0.199	0.64 ± 0.11	0.34 ± 0.20	45.2 ± 5.5	1.2	1.4	1.9
(e) Hamadori (Iwaki)	2.5	0.002 ± 0.002	1.35 ± 0.01	30 (fixed)	8,254 ± 528	169	219	326
(f) Choshi	3.0	0.002 ± 0.002	0.71 ± 0.02	1.15 ± 0.59	45.2 ± 6.3	2,303	3,858	7,420
(g) Tokyo Bay	1.2	0.057 ± 0.029	0.54 ± 0.04	0.00 ± 1.27	6.8 ± 1.6	12	20	39
(h) Izu-Hakone	2.0	0.720 ± 0.375	1.10 ± 0.08	0.09 ± 0.04	33.0 ± 4.7	0.07	0.09	0.12
(i) Central Nagano (ISTL)	0.6	0.699 ± 0.121	0.42 ± 0.02	20 (fixed)	23.0 ± 2.7	9.0	11.6	15.9
(j) Northern Nagano	1.6	0.103 ± 0.051	0.98 ± 0.02	0.28 ± 0.09	237 ± 17	6.1	7.5	10.0
(k) Kanto Seis. Corridor	3.0	0.157 ± 0.037	0.42 ± 0.05	2.38 ± 4.84	4.9 ± 1.4	2.8	4.4	7.7
(l) Tohoku source	5.0	0.036 ± 0.021	1.04 ± 0.02	0.04 ± 0.01	57.0 ± 4.1	2.6	3.2	4.4

In four cases (a, c, e, and i), (c) was fixed because it could not be stably inverted. ISTL, Itoigawa-Shizuoka Tectonic Line.

with the possible exception of Hamadori (Fig. 4e), all of the first shocks are small. The aftershock decays (p), background rates (r), and resulting estimated aftershock durations (t_a) are shown in Figure 5.

The estimated aftershock durations are given in Table 1, with well-determined durations from one month to 2000 years (compare Fig. 5h and 5f) and possibly much longer. Narteau *et al.* (2002) argued that the decay exponent could steepen after some period, but this is not evident in our data. The mean aftershock durations reflect the decay uncertainty but use only the mean background rate; the plus 1-sigma duration additionally incorporates the background rate uncertainty, which is not Gaussian because the rate must be positive. There is unique duration uncertainty in the Kanto seismic corridor beneath Tokyo (Toda *et al.*, 2008), which can be fit by a slower decay that will return to the background in about 10 years (Fig. 5k), or a 0.6-yr decay followed by a new higher background rate (gray curve) (Stein and Toda, 2013). A rigorous exploration of the Omori decay exponents and resulting aftershock durations is furnished in Ⓔ Tables S2–S13. (If the background rates were to change in the future by factors of more than about 5, the projected durations would themselves change appreciably.) It is important to note that the decay exponents p are generally about 1 (1.04 ± 0.61) and contribute relatively little to the aftershock decays.

Durations of Aftershocks of M_w 7–8 Mainshocks in Japan

The Japan Meteorological Agency (JMA) catalog supplies the world's largest number of $M_w \geq 7$ mainshocks with low completeness magnitudes and a long-enough record before the mainshocks to establish the background rate. Thus, we also calculate the aftershock durations for M_w 7.1–7.8 mainshocks from three tectonic settings along a Japan trench-normal transect (Fig. 6 and Table 2). For three events, the aftershock sequence has returned to the background rate. For three others, the decay continues, and we project their durations (three are shown in Fig. 6c; the others are in Tables 2 and 3 and Ⓔ Fig. S4). Finally, we consider two thrust mainshocks in the Japan Sea, the 25 May 1983 M_w 7.7 and 12 Jul 1993 M_w 7.8 events (Fig. 7), with observed aftershock durations of at least 20 yrs.

Particularly revealing is the comparison of three mainshocks from different tectonic environments with similar JMA 7.1–7.2 magnitudes and 0.9–1.0 Omori decay exponents in Figure 6. The background rate for the interplate event is 10 times higher than for the intraslab and inland earthquakes; the interplate event has an aftershock duration of 100–1000 days. For the other two events, aftershocks are projected to last for more than 30 yrs. The two earthquakes from the low-stressing-rate environments (the curves for inland M_w 7.2 and interplate M_w 7.1 in Fig. 6) have aftershock productivities (k-values) 10 times higher than the interplate event. Therefore, their aftershock sequences not only last much longer, they also produce about a hundred times more events. This accentuates the differences identified in Figure 2a and is the opposite of the case shown in Figure 2b.

Testing the Dependence of Aftershock Duration on Mainshock Magnitude and Slip Rate

Is there a relationship among aftershock duration and mainshock magnitude, fault-slip rate, or background seismicity rate? The fault-slip rate at aftershock sites is estimated from Research Group for Active Faults of Japan (1991). All slip rates and aftershock durations are tabulated in Table 3.

We find no correlation of aftershock duration with mainshock magnitude, regardless of whether we exclude the M_w 9 aftershocks (Fig. 8a). There is a modest inverse correlation of aftershock duration with fault-slip rate ($R^2 = 0.31$, and $R^2 = 0.61$ without the M_w 9 data; Fig. 8b) and a weak inverse correlation with background seismicity rate ($R^2 = 0.37$; Fig. 8c). Slip rate and background rate are proxies of stressing rate. Thus, the data suggest that an aftershock duration has a stronger dependence on

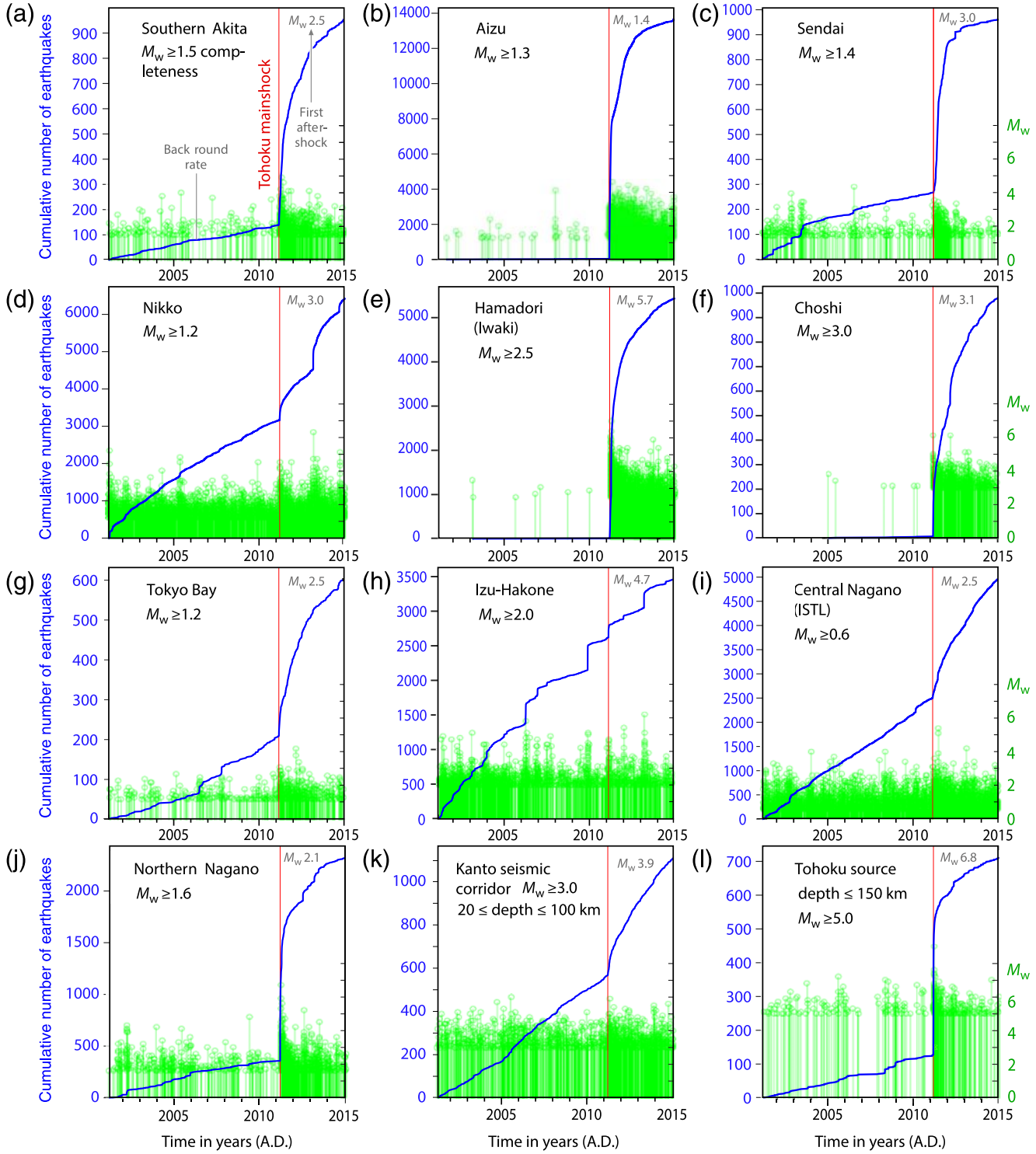

Figure 4. Cumulative time series of earthquakes above M_c, with each event shown as a stem. The abrupt increase in rate is evident in (a)–(l), except perhaps at (h) Izu-Hakone. (a–j) Seismicity at 0–20 km depth. In some cases, secondary aftershocks perturb the decay, but all show sudden rate increases at the time of the M_w 9 Tohoku mainshock. ISTL, Itoigawa-Shizuoka Tectonic Line. The color version of this figure is available only in the electronic edition.

stressing rate than it does on mainshock magnitude, consistent with Dieterich (1994). Although Hainzl *et al.* (2016) do not distinguish the tectonic regime of their California, New Zealand, and global mainshocks, they also find no magnitude correlation for true aftershock duration and a weak magnitude correlation for the apparent duration on which we focus in this study. As in this study, they find an inverse correlation with background seismicity rate.

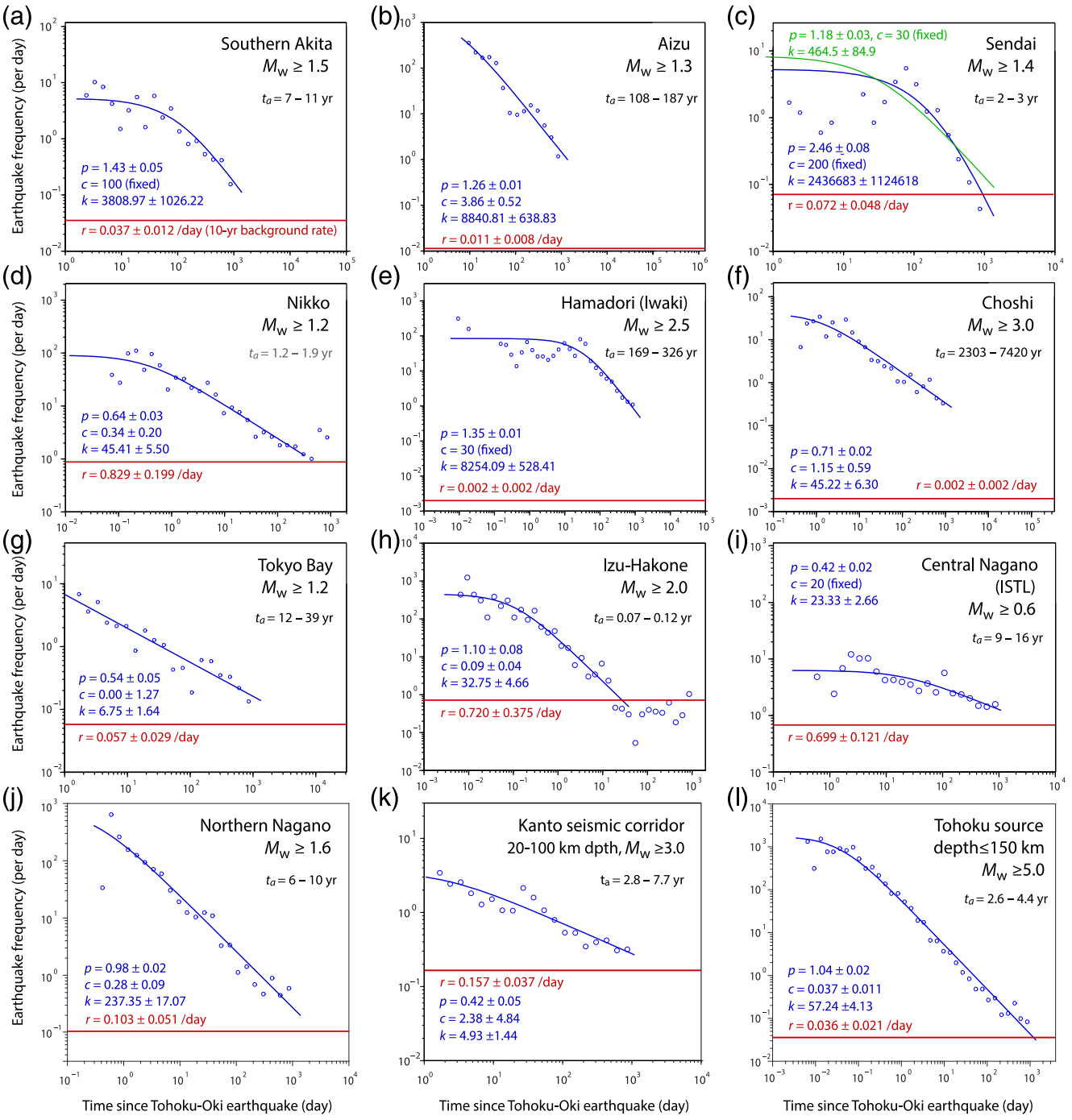

Figure 5. (a–l) Remote aftershock frequency decays (small circles) and 10-yr background rates. The intersection of the fitted curve with the background rate line gives the observed (c, d, and h) or projected (all others) aftershock durations (t_a), which are also given in Table 1. (e) The site of the M_w 7.0 Iwaki earthquake, which struck 30 days after the mainshock (Toda and Tsutsumi, 2013). The decay of seismicity at (d) Nikko is further explored in Ⓔ Table S5 and Figure S3. The decay in (k) the Kanto seismic corridor is explored in Ⓔ Table S12. The color version of this figure is available only in the electronic edition.

Conclusions and Implications for Seismic Hazard Assessment

Our strongest conclusion is that mainshock magnitude is not a dominant factor in observable aftershock duration. This is demonstrated by comparing remote aftershock sites of the M_w 9.0 Tohoku mainshock, for which observed or projected durations ranging from a month to at least a few centuries and perhaps millennia. It is also evident by comparing the near-fault aftershocks of mainshocks with the same magnitude (M_w 7.1–7.2), for which durations vary by two orders of magnitude. Even when we consider aftershocks restricted to

Table 2
Estimated Aftershock Durations of Large Earthquakes for Three Different Tectonic Settings

Date (yyyy/mm/dd)	M_{JMA}	Depth (km)	Type	Center of Sampling Cylinder (Longitude/ Latitude)	Radius of Cylinder (km)	Depth of Cylinder (km)	M_c	Starting Time for Background Seismicity (yr)	Background Seismicity Rate (/Day)	*p*-Value	*v*-Value	*k*-Value	t_a (yr)
1978/06/28	7.4	40	Interplate	142.15°/38.15°	40	0–150	3.5	1970	0.017	0.87 ± 0.05	0.00 ± 0.01	5.23 ± 0.96	2.1 ± 0.7
1994/12/28	7.6	0	Interplate	143.7°/40.4°	40	0–150	3.5	1985	0.035	0.94 ± 0.02	0.04 ± 0.02	30.69 ± 2.87	3.8 ± 0.7
2005/08/16	7.2	42	Interplate	142.15°/38.15°	40	0–150	2.0	1996	0.387	0.92 ± 0.03	0.00 ± 0.00	29.28 ± 2.00	0.31 ± 0.05
2003/05/26	7.1	72	Intraslab	141.65°/38.9°	20	40–150	2.0	1994	0.036	0.86 ± 0.01	0.02 ± 0.00	178.02 ± 6.08	54.5 ± 6.7
2005/11/15	7.2	45	Outer rise	144.7°/38.2°	30	0–150	2.8	1998	0.003	1.10 ± 0.02	0.25 ± 0.05	128.10 ± 10.61	45.2 ± 8.8
2008/06/14	7.2	8	Inland crustal	140.8°/39.0°	30	0–20	1.5	1998	0.197	0.93 ± 0.01	0.19 ± 0.02	818.28 ± 22.63	21.4 ± 2.2

JMA, Japan Meteorological Agency.

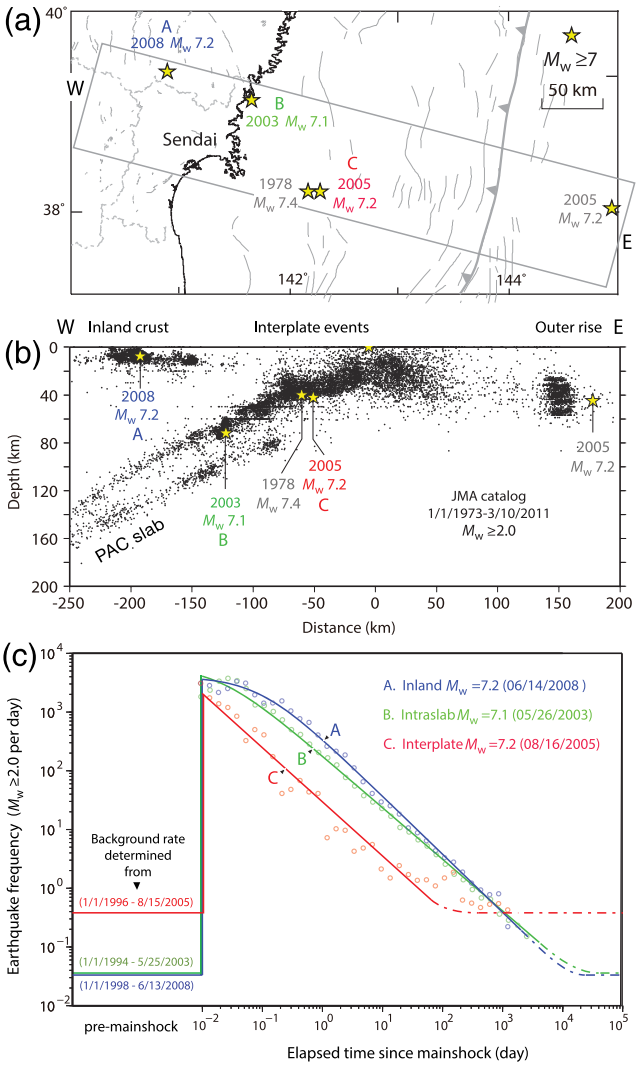

Figure 6. Recent $M_w \geq 7$ mainshocks, all of which struck before the M_w 9 Tohoku shock, in different stressing environments along a Japan trench-normal transect in (a) map view and (b) cross section. (c) Their aftershock frequency decays and durations are shown. The projected duration of the interplate (active tectonic) aftershock sequence is two orders of magnitude briefer than the others. The 16 August 2005 shock was analyzed by Okada *et al.* (2005). The color version of this figure is available only in the electronic edition.

the 2011 M_w 9.0 Tohoku rupture zone or the entire area of central Honshu in which isolated pockets of aftershocks are found (boxes l and m, respectively, in Fig. 3b,c), the durations are only approximately 3 yrs long, much shorter than the durations for many of the $M_w \geq 7$ mainshocks we examined in the more slowly deforming Japan Sea.

Our second conclusion is that aftershock duration could indeed be inversely proportional to fault stressing rate, as proposed by Dieterich (1994) and advocated by Ebel *et al.* (2000) and Stein and Liu (2009). Because the stressing rate cannot be directly measured, we infer a stressing-rate dependence from the correlation of aftershock duration with the fault-slip rate. Like most foregoing studies, we find that the Omori decay

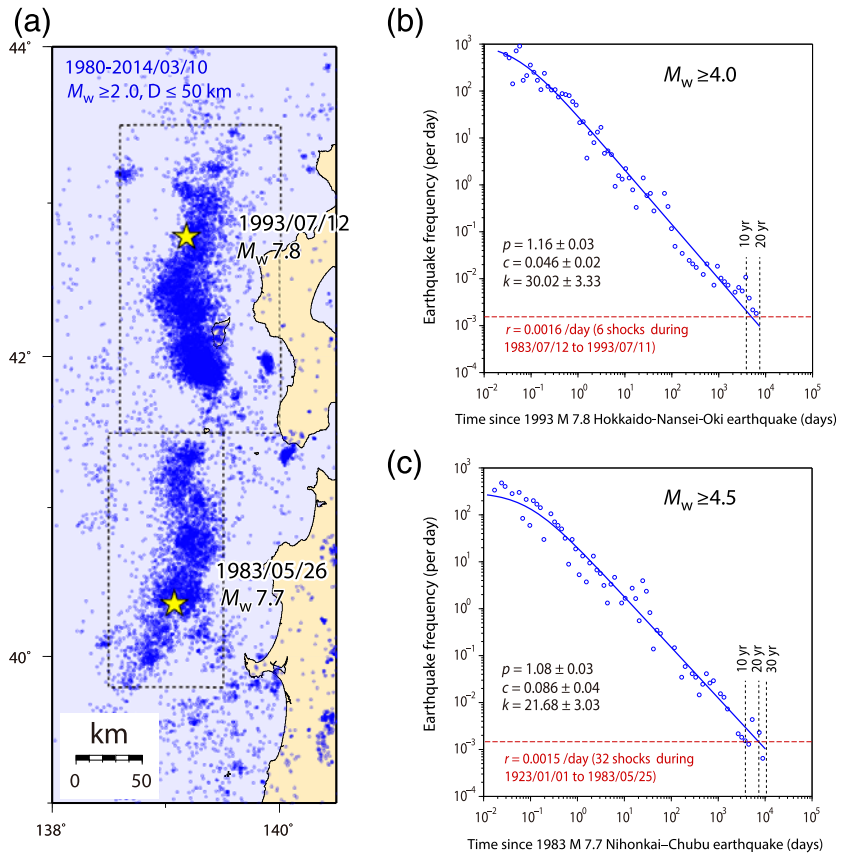

Figure 7. (a) Aftershock zones of the 25 May 1983 M_w 7.7 and the 12 July 1993 M_w 7.8 thrust earthquakes. (b,c) Decays of aftershocks at their magnitudes of completeness. The background rates are highly uncertain, but both sequences continue to decay. The color version of this figure is available only in the electronic edition.

exponent is about 1.0 for all but volcanic activity and swarms, indicating that the exponent exerts only a minor role on the range of aftershock durations.

Our third conclusion is that catalog declustering techniques (Gardner and Knopoff, 1974; Reasenberg, 1985; Molchan and Dmitrieva, 1992; van Stiphout *et al.*, 2012) are unlikely to remove aftershocks of long duration (tens to hundreds of years); thus, late aftershocks will tend to be misinterpreted as steady background seismicity. Only if one knows the seismicity rate for the decade before the mainshock would accurate aftershock removal be possible, as is seen from declustering the 1995–2016 M_w 6.9 Kobe aftershocks (Fig. 9). Hainzl *et al.* (2016) found that even when 100–500 background earthquakes before the mainshock were considered, only ETAS declustering was effective for 100 days for $M_w \sim 6$ mainshocks to 1000 days for $M_w \sim 7$ mainshocks. Because the ETAS parameters become more poorly determined for longer periods than these, a Poisson (nondecaying) fit performs better (Hainzl *et al.*, 2016). This means that even the most current techniques cannot contend with century-long aftershock sequences. Whether insufficient declustering leads to probabilistic seismic hazard assessments (PSHAs) that are too high or too low depends on the period considered relative to the seismicity-rate decay and on how much the assessment is driven by seismicity rates as opposed to fault-slip rates or geodetic strain rate. In places such as Australia and the eastern United States, assessments are driven by seismicity because fault-slip rates are either unknown or exceedingly low, and Global Positioning System-observed strain rates are either zero or dwarfed by nontectonic processes.

Implications for Seismic Hazards

The criteria commonly used for engineering purposes in seismic hazard assessments are 10% and 2% exceedance probabilities in 50 years, which correspond to the occurrence of earthquakes with interevent times of 475 and 2475 years, respectively, longer than most projected aftershock sequences in Table 3. Still longer interevent times are considered for nuclear facilities. For these long periods, if one scales up the rate of small shocks to forecast the rate of large ones, under the assumption that their rate is steady, the likelihood of large shocks would be greatly overestimated, as also argued by Liu and Wang (2012).

The hazard overestimation is schematically illustrated in Figure 10. Aftershocks are more common along or near the mainshock rupture, whereas future mainshocks are more likely to occur outside the previous mainshock rupture zone. After the mainshock, the probability of re-rupturing the fault in another mainshock is temporally reduced (Fig. 10b, solid curve) because the stress has dropped. However, in the same area, the rate of smaller shocks is temporally increased because along the periphery of the rupture, stress has increased (Fig. 10b, dashed curve).

Because PSHA generally considers larger destructive mainshocks, failure to recognize that the smaller events are aftershocks would thus yield too high an expected rate of larger shocks. Because long aftershock durations are more common in slowly deforming regions, this overestimate might be most acute in continental interiors and zones of diffuse deformation. As long as some aftershock sequences persist in a slowly deforming region, the average seismicity rate will always be higher than the background rate; thus, a hazard overestimate seems inevitable to us. That overestimate can be small or large, but not zero. The four $M_w \geq 7$ shocks in eastern North America in 350 years (Fig. 1a) suggest a rate of roughly one per century, and there is another half-dozen or so seismicity clusters in Figure 1a that could be the products of still older large mainshocks. If so, the roughly

Table 3
Estimated Aftershock Durations and Slip Rates for All Events in the Study

Figure Numbers	Identification of Aftershocks	Fault-Slip Rate (Mean, mm/yr)	Fault-Slip Rate (Minimum, mm/yr)	Fault-Slip Rate (Maximum, mm/yr)	Mainshock Magnitude (M_{JMA})	t_a 34th % (yr)	t_a 50th % (yr)	t_a 68th % (yr)	Slip Rate Ranges and Source References
3, 4, 5a	Southern Akita	1	0.3	3	9	7	9	11	~ 1.0 mm/yr, RGAF (1991) and HERP (2010), see Data and Resources
3, 4, 5b	Aizu	1	0.3	3	9	108	134	187	~ 1.0 mm/yr, RGAF (1991) and HERP (2010), see Data and Resources
3, 4, 5c	Sendai	0.6	0.5	0.7	9	2.1	2.7	3.4	0.5–0.7 mm/yr, RGAF (1991) and HERP (2010), see Data and Resources
3, 4, 5d	Nikko	1	0.1	1.5	9	1.2	1.4	1.9	<1.0 mm/yr, RGAF (1991) and HERP (2010), see Data and Resources
3, 4, 5e	Hamadori (Iwaki)	0.2	0.1	0.4	9	169	219	326	~ 0.2 mm/yr, Toda and Tsutsumi (2013)
3, 4, 5f	Choshi	0.2	0.1	0.4	9	2303	3858	7420	No mapped active fault; perhaps like Iwaki
3, 4, 5g	Tokyo Bay	—	—	—	9	12	20	39	No mapped active fault
3, 4, 5h	Izu-Hakone	2.5	2	3	9	0.07	0.09	0.12	2–3 mm/yr, volcanic, RGAF (1991) and HERP (2010), see Data and Resources
3, 4, 5i	Central Nagano (ISTL)	5	1	9	9	9	12	16	1–9 mm/yr, RGAF (1991) and HERP (2010), see Data and Resources
3, 4, 5j	Northern Nagano	1.9	1.2	2.6	9	6	8	10	1.2–2.6 mm/yr, RGAF (1991) and HERP (2010), see Data and Resources
3, 4, 5k	Kanto seismic corridor (20–100 km deep)	35	20	75	9	2.8	4.4	7.7	Toda *et al.* (2008)
3, 4, 5l	Tohoku source (0–150 km deep)	35	20	75	9	2.6	3.2	4.4	Assumes 50% coupling of 70 mm/yr convergence
6a	1978 interplate	40	30	70	7.4	1.4	2.1	2.9	Assumes 50% coupling of 80 mm/yr
Ⓔ S2a,b	1994 interplate	40	30	70	7.6	3.1	3.8	4.5	Assumes 50% coupling of 80 mm/yr
6a–c	2005 interplate	40	30	70	7.2	0.26	0.31	0.36	Assumes 50% coupling of 80 mm/yr
6a–c	2003 Intraplate	2	1	3	7.1	47.8	54.5	61.2	Assumes a typical slip rate of most active crustal faults
6a, Ⓔ S2c,d	2005 outer rise	2	1	3	7.2	36.4	45.2	54	Assumes a typical slip rate of most active crustal faults
6a–c	2008 inland crustal	0.4	0.1	0.5	7.2	19.2	21.4	23.6	0.1–0.4 mm/yr, Toda *et al.* (2011) and HERP (2010), see Data and Resources
7a,b	1993 Hokkaido-Nansei-Oki	4.1	2.4	5.8	7.8	20	21	41	Loveless and Meade (2010), assuming 50% coupling
7a,b	1983 Nihonkai–Chubu	6.9	5.8	8	7.7	30	31	51	Loveless and Meade (2010)

HERP, Headquarters for Earthquake Research Promotion; RGAF, Research Group for Active Faults of Japan.

10 clusters might reflect large earthquakes extending back approximately 1000 years.

Could this problem be reduced by the use of geodesy or paleoseismology? Very few national PSHA models balance the seismic moment against the geodetic moment. Even if they do, there is a factor-of-two uncertainty in the effective elastic thickness needed to convert surface strain rates into seismic moment rates and another factor of two in the earthquake rate associated with the assumed magnitude–frequency relationship. Further, for slowly deforming regions where long aftershocks durations are most common, the geodetic strain rate is either too small to detect, as is arguably the case for New Madrid (Craig and Calais, 2014), or is swamped by postglacial rebound (central and northern United States, central and eastern Canada, and central and northern Europe). Therefore, paleoseismology is crucial to determine whether a seismicity cluster could be aftershocks of a prehistoric mainshock (Leonard *et al.*, 2007).

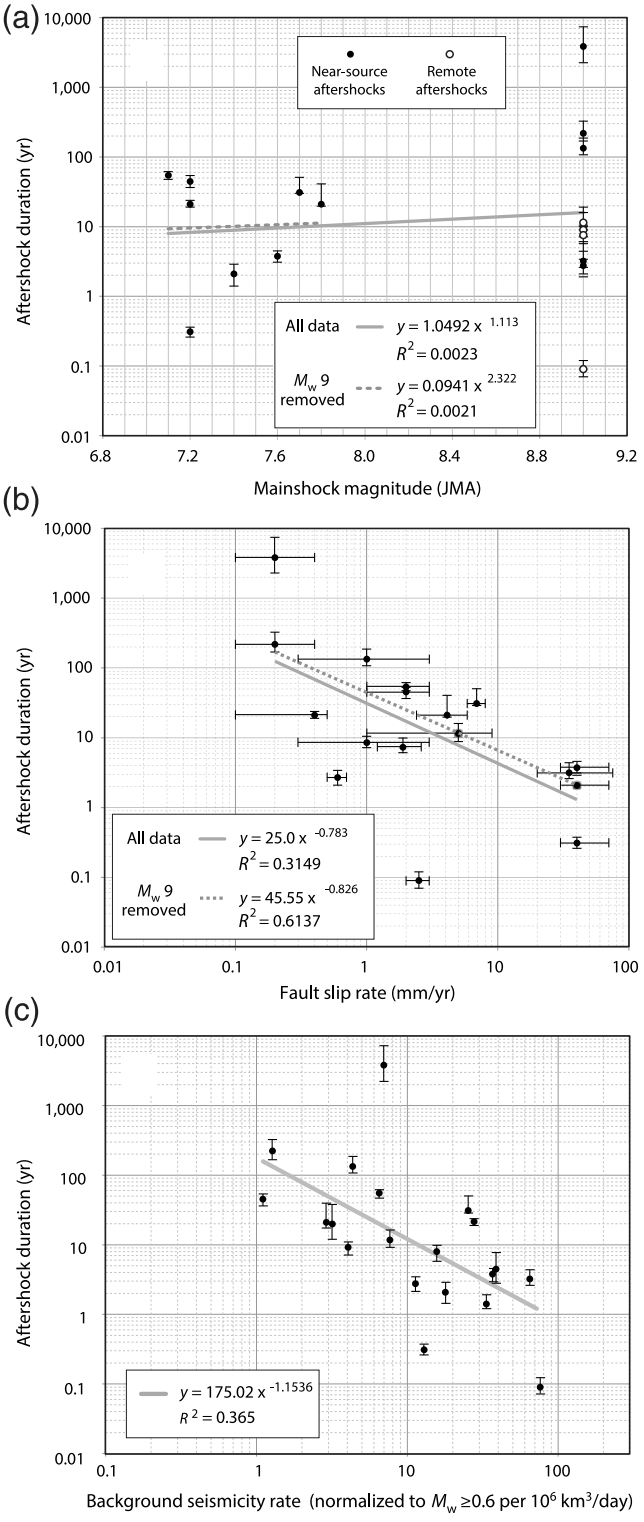

Figure 8. Aftershock duration as a function of (a) mainshock magnitude, (b) fault-slip rate, and (c) background seismicity rate normalized to $M_w \geq 0.6$ by assuming $b = 1.0$, all with their respective correlation coefficients. Remote aftershocks lie > 250 km from the M_w 9 epicenter and > 200 km from the closest edge of the rupture surface. One sees no magnitude dependence, but there are inverse dependences on fault-slip rate and background seismicity rate.

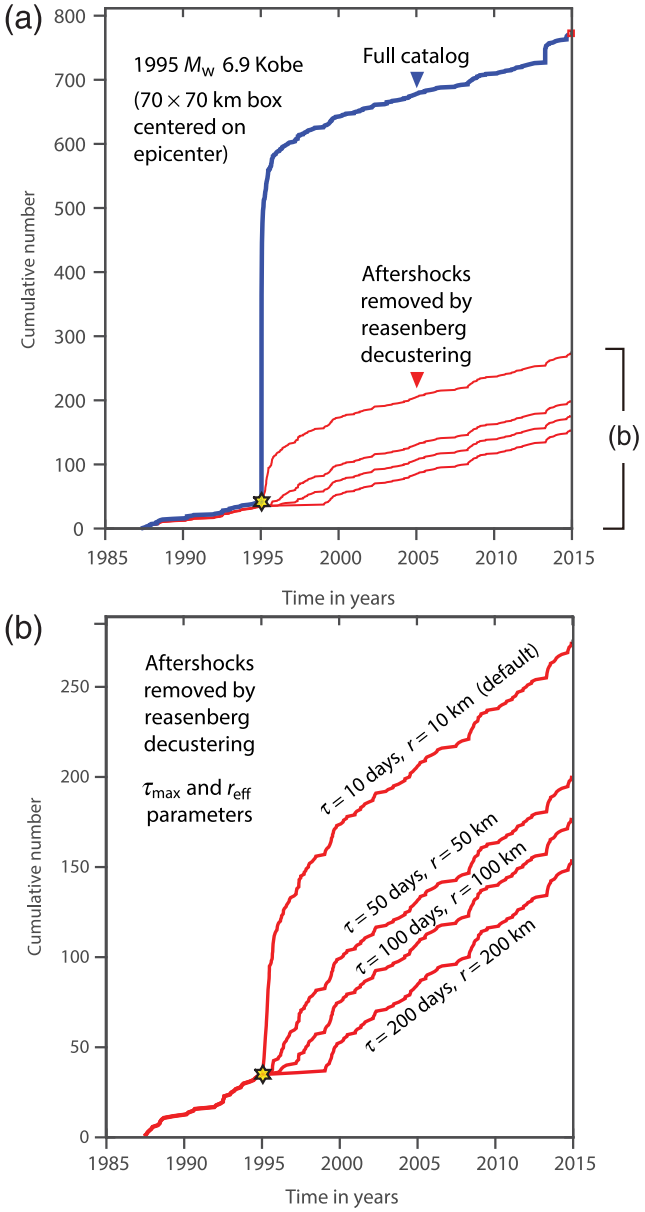

Figure 9. (a) Time series of seismicity from the original Japan Meteorological Agency (JMA) catalog and declustered catalogs for the 1995 Kobe earthquake, above the $M_c = 2.6$ completeness magnitude as determined by Toda *et al.* (1998). (b) Magnified plot of the declustered cumulative curves. Removing aftershocks of the long-lived Kobe earthquake sequence using standard declustering techniques is possible only if the seismicity time series starts well before the mainshock, and one can fit the declustering parameters. This would fail altogether if the mainshock struck long before the seismicity time series began or if only the standard parameters were used. The color version of this figure is available only in the electronic edition.

A limitation of our analysis is that we assumed that there is such a thing as background seismicity, events are not themselves aftershocks. At best, this can only be partially correct because most shocks produce aftershocks, and this process is

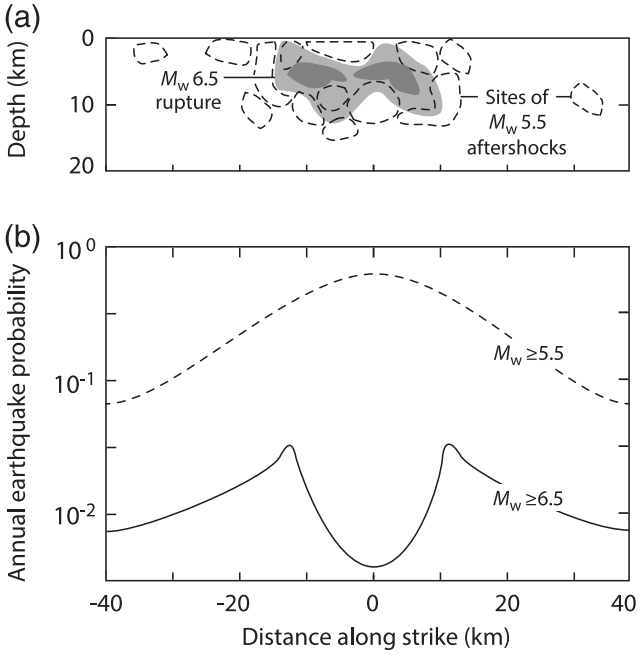

Figure 10. (a) Schematic M_w 6.5 rupture area and typical sites of potential large aftershocks. (b) Earthquake probabilities during the aftershock sequence, with a reduced likelihood of an M_w 6.5 earthquake within the recent rupture area. Subsequent M_w 6.5 shocks will most likely nucleate at the periphery of the past rupture for which the probability is the highest.

scale independent. Further, even for the San Andreas fault, for which the slip rate is fairly uniform over its 1000-km length, the background seismicity along the fault is highly variable, making the current background rate alone unable to reflect the fault stressing rate. Finally, the long (>30-yr) aftershock durations in our study are projected, not measured. Despite these limitations, when aftershock durations are objectively estimated, they last from months to millennia, with the longest durations associated with the lowest rates of tectonic deformation and fault slip.

Data and Resources

The Japan Meteorological Agency (JMA) hypocenter data files are accessible from http://www.data.jma.go.jp/svd/eqev/data/bulletin/index_e.html (last accessed September 2017). The unified earthquake catalog of the JMA was accessed via the University of Tokyo FTP site, and the same data set is publicly available from http://wwweic.eri.u-tokyo.ac.jp/db/jma.deck/index-j.html (last accessed September 2017) and http://www.data.jma.go.jp/svd/eqev/data/bulletin/index_e.html (last accessed September 2017). MATLAB software packages ZMAP (http://www.seismo.ethz.ch/static/stat_2010_website/stat-website-pre2010/www.earthquake.ethz.ch/docs/papers/wiemer2001.html, last accessed September 2017) and Coulomb (https://pubs.usgs.gov/of/2011/1060/, last accessed September 2017) were used to analyze seismicity and Coulomb stress change, respectively. Epidemic-type aftershock sequence (ETAS) analyses for the aftershocks were done using the SASeis2006 software (http://www.ism.ac.jp/~ogata/Ssg/ssg_softwares.html, last accessed September 2017). We used the Headquarters for Earthquake Research Promotion (HERP) (2010), National seismic hazard maps for Japan 2010, Earthquake Research Committee (K. Abe, chair), Headquarters for Earthquake Research Promotion, available at www.jishin.go.jp/main/chousa/10_yosokuchizu/index.htm (last accessed January 2018) (in Japanese).

Acknowledgments

The authors thank Gail Atkinson, Sebastian Hainzl, Ruth Harris, Morgan Page, Fred Pollitz, and Seth Stein for comprehensive reviews.

References

Basham, P., and J. Adams (1983). Earthquakes on the continental margin of eastern Canada: Need future large events be confined to the locations of large historical events? in W. W. Hays and P. L. Gori, *U.S. Geol. Surv. Open-File Rept. 83-843*, 456–467.

Choy, G. L., and J. R. Bowman (1990). Rupture process of a multiple main shock sequence: Analysis of teleseismic, local, and field observations of the Tennant Creek, Australia, earthquakes of January 22, 1988, *J. Geophys. Res.* **95,** 6867–6882, doi: 10.1029/JB095iB05p06867.

Clark, D., and K. McCue (2003). Australian paleoseismology: Towards a better basis for seismic hazard estimation, *Ann. Geophys.* **46,** 1087–1105.

Craig, T. J., and E. Calais (2014). Strain accumulation in the New Madrid and Wabash Valley seismic zones from 14 years of continuous GPS observation, *J. Geophys. Res.* **119,** 9110–9129, doi: 10.1002/2014JB011498.

Dieterich, J. (1994). A constitutive law for rate of earthquake production and its application to earthquake clustering, *J. Geophys. Res.* **99,** 2601–2618.

Ebel, J. E. (2016). Comment on "Aftershock Statistics for Earthquakes in the St. Lawrence Valley" by Azadeh Fereidoni and Gail M. Atkinson, *Seismol. Res. Lett.* **87,** 149–151, doi: 10.1785/0220150120.

Ebel, J. E., K.-P. Bonjer, and M. C. Oncescu (2000). Paleoseismicity: Seismicity evidence for past large earthquakes, *Seismol. Res. Lett.* **71,** 283–294.

Felzer, K. R., R. E. Abercrombie, and G. Ekström (2004). A common origin for aftershocks, foreshocks, and multiplets, *Bull. Seismol. Soc. Am.* **94,** 88–98, doi: 10.1785/0120030069.

Fereidoni, A., and G. M. Atkinson (2014). Aftershock statistics for earthquakes in the St. Lawrence valley, *Seismol. Res. Lett.* **85,** 1125–1136.

Fereidoni, A., and G. M. Atkinson (2016). Reply to "Comment on 'Aftershock Statistics for Earthquakes in the St. Lawrence Valley' by Azadeh Fereidoni and Gail M. Atkinson" by John Ebel, *Seismol. Res. Lett.* **87,** 152–156, doi: 10.1785/0220150170.

Gardner, J. K., and L. Knopoff (1974). Is the sequence of earthquakes in Southern California, with aftershocks removed, Poissonian? *Bull. Seismol. Soc. Am.* **64,** 1363–1367.

Hainzl, S., A. Christophersen, D. Rhoades, and D. Harte (2016). Statistical estimation of the duration of aftershock sequences, *Geophys. J. Int.* **205,** 1180–1189, doi: 10.1093/gji/ggw075.

Harris, R. A. (1998). Introduction to special section: Stress triggers, stress shadows, and implications for seismic hazard, *J. Geophys. Res.* **103,** 24,347–324,358.

Iinuma, T., R. Hino, M. Kido, D. Inazu, Y. Osada, Y. Ito, M. Ohzono, H. Tsushima, S. Suzuki, H. Fujimoto, *et al.* (2012). Coseismic slip distribution of the 2011 off the Pacific Coast of Tohoku earthquake (M 9.0) refined by means of seafloor geodetic data, *J. Geophys. Res.* **117,** doi: 10.1029/2012JB009186.

Jonsson, S., P. Segall, R. Pedersen, and G. Bjornsson (2003). Post-earthquake ground movements correlated to pore-pressure transients, *Nature* **424,** 179–183.

Leonard, M., D. Burbidge, and M. Edwards (2013). Atlas of seismic hazard maps of Australia: Seismic hazard maps, hazard curves and hazard spectra, *Record 2013/41*, Geoscience Australia, Canberra, Australia.

Leonard, M., D. Robinson, T. Allen, J. Schneider, D. Clark, T. Dhu, and D. Burbidge (2007). Toward a better model of earthquake hazard in Australia, *Geol. Soc. Am. Spec. Pap.* **425,** 263–283, doi: 10.1130/2007.2425(17).

Liu, M., and H. Wang (2012). Roaming earthquakes in China highlight midcontinental hazards, *Eos Trans. AGU* **93,** no. 45, 453–454, doi: 10.1029/2012EO450001.

Loveless, J. P., and B. J. Meade (2010). Geodetic imaging of plate motions, slip rates, and partitioning of deformation in Japan, *J. Geophys. Res.* **115,** no. B02410, doi: 10.1029/2008JB006248.

Molchan, G. M., and O. E. Dmitrieva (1992). Aftershock identification: Methods and new approaches, *Geophys. J. Int.* **109,** 501–516, doi: 10.1111/j.1365-246X.1992.tb00113.x.

Narteau, C., P. Shebalin, and M. Holschneider (2002). Temporal limits of the power law aftershock decay rate, *J. Geophys. Res.* **107,** 2359, doi: 10.1029/2002JB001868.

Ogata, Y. (1998). Space-time point-process models for earthquake occurrences, *Ann. Inst. Stat. Math.* **50,** 379–402.

Okada, T., T. Yaginuma, N. Umino, T. Kono, T. Matsuzawa, S. Kita, and A. Hasegawa (2005). The 2005 M 7.2 Miyaki-Oki earthquake, NE Japan: Possible rerupturing of one of asperities that caused the previous M 7.4 earthquake, *Geophys. Res. Lett.* **32,** L24302, doi: 10.1029/2005GL024613.

Omori, F. (1894). On the aftershocks of earthquakes, *J. Coll. Sci. Imp. Univ. Tokyo* **7,** 111–200.

Page, M. T., and S. E. Hough (2014). The New Madrid Seismic Zone: Not dead yet, *Science* **343,** 762–764, doi: 10.1126/science.1248215.

Parsons, T. (2002). Global Omori law decay of triggered earthquakes: Large aftershocks outside the classical aftershock zone, *J. Geophys. Res.* **107,** 2199, doi: 10.1029/2001JB000646.

Reasenberg, P. (1985). Second-order moment of central California seismicity, 1969–1982, *J. Geophys. Res.* **90,** 5479–5495.

Research Group for Active Faults of Japan (RGAF) (1991). *Active Faults in Japan, Sheet Maps and Inventories*, Revised Ed., University of Tokyo Press, Tokyo, Japan, 437 pp.

Schlupp, A., and A. Cisternas (2007). Source history of the 1905 great Mongolian earthquakes (Tsetserleg, Bolnay), *Geophys. J. Int.* **169,** 1115–1131, doi: 10.1111/j.1365-246X.2007.03323.x.

Stein, R. S., and S. Toda (2013). Megacity megaquakes—Two near misses, *Science* **341,** 850–852, doi: 10.1126/science.1238944.

Stein, S., and M. Liu (2009). Long aftershock sequences within continents and implications for earthquake hazard assessment, *Nature* **462,** 87–89, doi: 10.1038/nature08502.

Stein, S., and A. Newman (2004). Characteristic and uncharacteristic earthquakes as possible artifacts: Applications to the New Madrid and Wabash seismic zones, *Seismol. Res. Lett.* **75,** 173–187.

Toda, S., and R. S. Stein (2002). Response of the San Andreas fault to the 1983 Coalinga-Nuñez earthquakes: An application of interaction-based probabilities for Parkfield, *J. Geophys. Res.* **107,** doi: 10.1029/2001JB000172.

Toda, S., and R. S. Stein (2003). Toggling of seismicity by the 1997 Kagoshima earthquake couplet: A demonstration of time-dependent stress transfer, *J. Geophys. Res.* **108,** 2567, doi: 10.1029/2003JB002527.

Toda, S., and H. Tsutsumi (2013). Simultaneous reactivation of two, subparallel, inland normal faults during the M_w 6.6 11 April 2011 Iwaki earthquake triggered by the M_w 9.0 Tohoku-Oki, Japan, earthquake, *Bull. Seismol. Soc. Am.* **103,** 1584–1602, doi: 10.1785/0120120281.

Toda, S., R. S. Stein, S. H. Kirby, and S. B. Bozkurt (2008). A slab fragment wedged under Tokyo and its tectonic and seismic implications, *Nature Geosci.* **1,** 771–776, doi: 10.1038/ngeo318.

Toda, S., R. S. Stein, and J. Lin (2011). Widespread seismicity excitation throughout central Japan following the 2011 M = 9.0 Tohoku earthquake and its interpretation by Coulomb stress transfer, *Geophys. Res. Lett.* **38,** L00G03, doi: 10.1029/2011GL047834.

Toda, S., R. S. Stein, P. A. Reasenberg, and J. H. Dieterich (1998). Stress transferred by the M_w 6.9 Kobe, Japan, shock: Effect on aftershocks and future earthquake probabilities, *J. Geophys. Res.* **103,** 24,543–24,565, doi: 10.1029/98JB00765.

Toda, S., R. S. Stein, J. Richards-Dinger, and S. B. Bozkurt (2005). Forecasting the evolution of seismicity in southern California: Animations built on earthquake stress transfer, *J. Geophys. Res.* **110,** no. B05S16, doi: 10.1029/2004JB003415.

Toda, S, R. S. Stein, and T. Sagiya (2002). Evidence from the AD 2000 Izu islands earthquake swarm that stressing rate governs seismicity, *Nature* **419,** 58–61. doi: 10.1038/nature00997.

Utsu, T., Y. Ogata, and R. Matsu'ura (1995). The centenary of the Omori formula for a decay law of aftershock activity, *J. Phys. Earth* **43,** 1–33.

van Stiphout, T., J. Zhuang, and D. Marsan (2012). Seismicity declustering, *Comm. Online Resour. Stat. Seism. Anal.*, doi: 10.5078/corssa-52382934.

Woessner, J., and S. Wiemer (2005). Assessing the quality of earthquake catalogues: Estimating the magnitude of completeness and its uncertainty, *Bull. Seismol. Soc. Am.* **95,** 684–698.

Ziv, A. (2006). Does aftershock duration scale with mainshock size? *Geophys. Res. Lett.* **33,** L17317, doi: 10.1029/2006GL027141.

International Research Institute of Disaster Science (IRIDeS)
Tohoku University
Aoba, 468-1, Aoba
Sendai 980-0845, Japan
toda@irides.tohoku.ac.jp
(S.T.)

U.S. Geological Survey
345 Middlefield Road, MS 977
Menlo Park, California 94025
rstein@usgs.gov
(R.S.S.)

Manuscript received 21 September 2017;
Published Online 1 May 2018